Conversion of E_4 ($E_4 = P_4$, As_4, AsP_3) by Ni(0) and Ni(I) Synthons – A Comparative Study

Maria Haimerl,[a] Christian Graßl,[a] Michael Seidl,[a] Martin Piesch,[a] and Manfred Scheer*[a]

Dedicated to Professor Rainer Anwander on the occasion of his 60th birthday.

Abstract: The reactivity of white phosphorus and yellow arsenic towards two different nickel nacnac complexes is investigated. The nickel complexes [$(L^1Ni)_2$tol] (**1**, L^1 = [{N($C_6H_3{}^iPr_2$-2,6)C(Me)}$_2$CH]$^-$) and [K_2][$(L^1Ni)_2(\mu,\eta^{1:1}$-$N_2)$] (**6**) were reacted with P_4, As_4 and the interpnictogen compound AsP_3, respectively, yielding the homobimetallic complexes [$(L^1Ni)_2(\mu$-η^2,κ^1:η^2,κ^1-$E_4)$] (E = P (**2a**), As (**2b**), AsP_3 (**2c**)), [$(L^1Ni)_2(\mu,\eta^{3:3}$-$E_3)$] (E = P (**3a**), As (**3b**)) and [K@18-c-6(thf)$_2$][$L^1Ni(\eta^{1:1}$-$E_4)$] (E = P (**7a**), As (**7b**)), respectively. Heating of **2a**, **2b** or **2c** also leads to the formation of **3a** or **3b**. Furthermore, the reactivity of these compounds towards reduction agents was investigated, leading to [K_2][$(L^1Ni)_2(\mu,\eta^{2:2}$-$P_4)$] (**4**) and [K@18-c-6(thf)$_3$][$(L^1Ni)_2(\mu,\eta^{3:3}$-$E_3)$] (E = P (**5a**), As (**5b**)), respectively. Compound **4** shows an unusual planarization of the initial Ni_2P_4-prism. All products were comprehensively characterized by crystallographic and spectroscopic methods.

Introduction

The activation of small molecules under mild conditions is an important topic in current research, because it can contribute to future energy conversions.[1] Besides Cp^R coordinating transition metal complexes, also low valent metal complexes stabilized by β-diiminato ligands[2] are adequate precursors for the reductive activation of small molecules such as N_2, O_2 or S_8,[3] but also for P_4 and As_4.[4] For the latter, by different reaction conditions such as photolysis or thermolysis, a broad variety of metal complexes with different polypnictogen moieties could be synthesized. With main group metal complexes of group 13, Roesky et al. reported the dinuclear aluminum complex [$(L^1Al)_2(\mu,\eta^{1:1:1:1}$-$P_4)$] (**A**, L^1 = [{N($C_6H_3{}^iPr_2$-2,6)C(Me)}$_2$CH]$^-$, Scheme 1) which contains a P_4^{4-} unit.[4a] The reaction of the corresponding Ga(I) complex [L^1Ga] with P_4 leads to [$L^1Ga(\eta^{1:1}$-$P_4)$] and other polyphosphine-containing complexes.[4b,k] In the area of transition metal complexes, only few examples of the early transition metals of Group 5 are known, for example the neutral vanadium complex [{L^1V(Ntolyl$_2$)}$_2(\mu,\eta^{3:2}$-$P_3)$] (**B**, Scheme 1)[4d] containing a *cyclo*-$[P_3]^{3-}$ ligand or the dinuclear complexes [{L^1(N^{t}Bu)M}$_2(\mu,\eta^{3:3}$-$P_4)$] (M = Nb, Ta)[4e] with a bridging *cyclo*-P_4 unit in an $\eta^{3:3}$ coordination mode. In contrast, during the last decade, for late Group 8–11 transition metals, numerous examples were reported. For cobalt and iron complexes, systematic studies with different nacnac ligands were performed leading to various E_n units (n = 3, 4 and 8) depending on the steric and electronic influence of the nacnac ligand.[4j,l–n] Driess et al. first synthesized the dinuclear iron complex [$(L^2Fe)_2(\mu,\eta^{2:2}$-$P_2)_2$] (**C**; L^2 = [{N($C_6H_3{}^iPr_2$-2,6)C(H)}$_2$CH]$^-$)), which contains two anionic P_2 ligands. An analogues arsenic derivative has also been reported.[4n] By using nacnac systems with less steric flanking groups, the tetranuclear complexes [$(L^{3/4}Fe)_4(\mu,\eta^{2:2:2:2}$-$E_8)$] (**D1-D4**; E = P, As; L^3 = [{N(C_6H_3Me-2,6)C(Me)}$_2$CH]$^-$ or L^4 = [{N(C_6H_3Me-2,6)C(H)}$_2$CH]$^-$)[4j,n] could be synthesized. These E_8 units display a realgar-type geometry.[5] Interestingly, the activation of white phosphorus by [LCo(tol)] (L = L^1, L^2, L^3, L^4) leads to the sole formation of [$(LCo)_2(\mu,\eta^{4:4}$-$P_4)$],[4l,6] however, the reaction with yellow arsenic yields complexes containing different {Co_2As_4} cores.[4m] Recently, we were able to synthesize and characterize the first neutral and

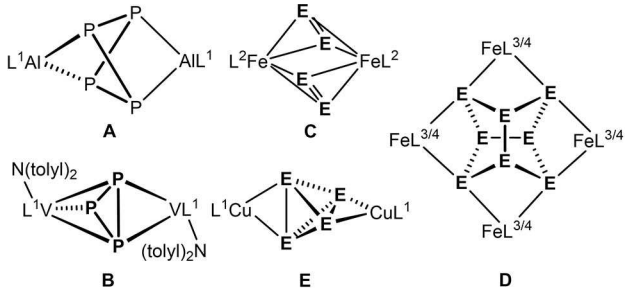

Scheme 1. Examples of known motifs of E_n ligand complexes stabilized by β-diketiminato ligands (L^1 = [{N($C_6H_3{}^iPr_2$-2,6)C(Me)}$_2$CH]$^-$, L^2 = [{N($C_6H_3{}^iPr_2$-2,6)C(H)}$_2$CH]$^-$, L^3 = [{N(C_6H_3Me-2,6)C(Me)}$_2$CH]$^-$ or L^4 = [{N(C_6H_3Me-2,6)C(H)}$_2$CH]$^-$; D1 = L^3, P; D2 = L^3, As; D3 = L^4, P; D4 = L^4, As)

[a] M. Haimerl, Dr. C. Graßl, Dr. M. Seidl, Dr. M. Piesch, Prof. Dr. M. Scheer
Institute for Inorganic Chemistry
University of Regensburg
Universitätsstraße 31, 93053 Regensburg (Germany)
E-mail: Manfred.Scheer@ur.de

Supporting information for this article is available on the WWW under https://doi.org/10.1002/chem.202103372

molecular complex containing an intact E_4 tetrahedron, for example, $[(L^1Cu)_2(\mu,\eta^{2:2}\text{-}E_4)]$[4h] (E = P (**E1**), As (**E2**)) (Scheme 1), which is easy to handle (neither flammable nor light-sensitive) and can release E_4 in a controlled manner.

For β-diiminato complexes of Ni, the Driess group used the Ni(I) synthon $[(L^1Ni)_2tol]$ (**1**) to activate small molecules such as H_2, N_2[7] and chalcogens (O_2, S_8, Se and Te).[3e,8] The reaction of **1** with white phosphorus leads only to $[(L^1Ni)_2(\mu\text{-}\eta^2{:}\eta^1,\kappa^1{:}\eta^2,\kappa^1\text{-}P_4)]$ containing a Ni_2P_4 prism, from which an $\{L^1Ni\}$ fragment can be released in solution.[4c] Inspired by the different reaction outcome, in the case of Fe(I) and Co(I) nacnac complexes and the coordination of the intact E_4 moiety in the case of Cu(I) nacnac complexes, the question arose as to what would happen in the case of nickel nacnac compounds. Would a different reaction behavior occur between phosphorus and arsenic? Moreover, the reactivity of an already reduced nickel species as a formal Ni(0) synthon towards white phosphorus and yellow arsenic was of interest to explore if there are similarities or differences towards the reaction of the respective Ni(I) nacnac species with E_4. Furthermore, since only a few reactions of the interpnictogen compound AsP_3 are reported, we targeted to include this species in this research.

Herein we report on the reactivity of $[(L^1Ni)_2tol]$ (L^1 = $[\{N(C_6H_3{}^iPr_2\text{-}2,6)C(Me)\}_2CH]^-$) towards white phosphorus, yellow arsenic and AsP_3. The reaction of **1** with E_4 leads to two different species depending on the used temperature, $[(L^1Ni)_2(\mu\text{-}\eta^2,\kappa^1{:}\eta^2,\kappa^1\text{-}E_4)]$ and $[(L^1Ni)_2(\mu,\eta^{3:3}\text{-}E_3)]$. Further reduction of these products leads to novel anionic dinuclear species with an $\eta^{2:2}$ *cyclo*-P_4 unit or $\eta^{3:3}$ *cyclo*-E_3 units. Moreover, reactions of the formally Ni(0) species $[K_2][(L^1Ni)_2(\mu,\eta^{1:1}\text{-}N_2)]$ with white phosphorus and yellow arsenic give unique anionic mononuclear compounds bearing an E_4 butterfly ligand.

Results and Discussion

The reaction of $[(L^1Ni)_2tol)]$ (**1**) with P_4 at −78 °C leads to the sole formation of the already reported $[(L^1Ni)_2(\mu\text{-}\eta^2,\kappa^1{:}\eta^2,\kappa^1\text{-}P_4)]$ (**2a**).[4c] Performing the reaction of **1** with E_4 in toluene at room temperature (to allow a high content of As_4) leads to the formation of $[(L^1Ni)_2(\mu\text{-}\eta^2,\kappa^1{:}\eta^2,\kappa^1\text{-}E_4)]$ ($E_4 = As_4$ (**2b**), AsP_3 (**2c**); Scheme 2). In contrast, the reaction of **1** with E_4 at +60 °C yields $[(L^1Ni)_2(\mu,\eta^{3:3}\text{-}E_3)]$ (E = P (**3a**), As (**3b**)) (Scheme 2).

2b, **2c**, **3a** and **3b** are obtained as greenish-brown (**2b**, **3b**) or green (**2c**, **3a**) air-sensitive solids in isolated yields of 38% (**2b**), 23% (**2c**), 44% (**3a**) and 81% (**3b**). Obviously, the slightly higher temperature triggers a release of an E atom of the otherwise formed prismane-like structure. This can also be observed by refluxing a toluene solution of **2a**, **2b** or **2c** for 2 h leading to the complete conversion to **3a** (for **2a** and **2c**) and **3b**, which was monitored by $^{31}P\{^1H\}$ and ^1H NMR spectroscopy. By further reduction of **2a**, **2b**,[9] **3a** and **3b** with KC_8, the compounds $[K_2][(L^1Ni)_2(\mu,\eta^{2:2}\text{-}P_4)]$ (**4**) and $[(K@18\text{-}c\text{-}6)thf)_3][(L^1Ni)_2(\mu,\eta^{3:3}\text{-}E_3)]$ (E = P (**5a**), As (**5b**)), respectively, were obtained in crystalline yields of 17% (**4**), 27% (**5a**) and 53% (**5b**) (Scheme 2). **4** shows an interesting planarization to a *cyclo*-P_4^{2-} moiety, whereas the pseudo-triple decker compounds **3a** and **3b** retain their structures.

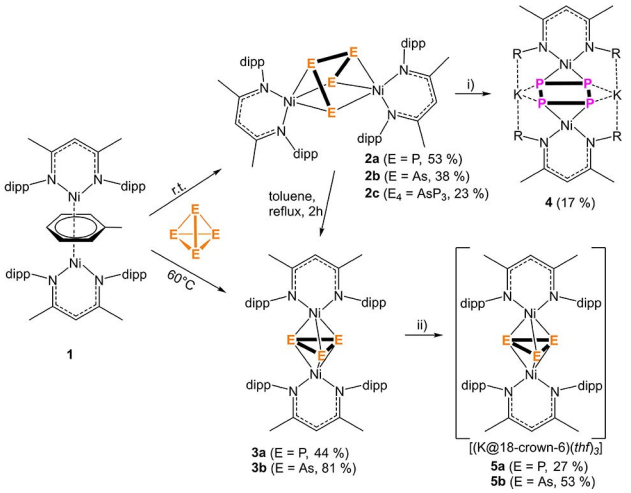

Scheme 2. Reaction of **1** with E_4 (E = P, As) and further reduction (R = dipp = 2,6-diisopropylphenyl). i) KC_8, toluene; ii) KC_8 + 18-crown-6, thf.

The ^1H NMR spectrum of **2a** shows a paramagnetic behavior in solution but is diamagnetic in the solid state and, accordingly, the $^{31}P\{^1H\}$ NMR spectrum is silent.[4c] In contrast, the ^1H NMR spectra of **2b** and **2c** at room temperature display one set of signals for the equivalent nacnac ligands. The $^{31}P\{^1H\}$ NMR spectrum of the reaction solution of **2c** in toluene-d_8 exhibits two broad signals at δ = 226.2 and 125.0 ppm, with an integral ratio of 1:2. Compounds **3a** and **3b** are paramagnetic. Their ^1H NMR spectra show broad and very shifted signals between 12.67 and −25.13 ppm for **3a** and between 12.01 and −23.31 ppm for **3b**. The $^{31}P\{^1H\}$ NMR spectrum of **3a** is silent because of an excessive line broadening. The effective magnetic moment (μ_{eff}) was determined by the Evans method to be 2.12 μ_B (**3a**) and 2.13 μ_B (**3b**), respectively, roughly corresponding to one unpaired electron. The X-band EPR spectra confirm the paramagnetic nature of **3a** and **3b** (frozen toluene solution, 77 K: **3a**: g_1 = 2.254, g_2 = 2.108 and g_3 = 2.063; **3b**: g_1 = 2.2705, g_2 = 2.135, g_3 = 2.055). At 77 K, the EPR spectrum of **3a** displays a hyperfine coupling to two phosphorus nuclei (Figure 1). DFT calculations (B3LYP/def2-SVP level) show that the spin density is delocalized over both nickel atoms and two phosphorus atoms (Figure 1) agreeing with the observed hyperfine coupling. The $^{31}P\{^1H\}$ NMR spectrum of **4** in C_6D_6 shows one singlet at δ = 80.3 ppm. Due to a dynamic behavior, **5a** reveals no signal at room temperature but a singlet at δ = −268.9 ppm in thf-d_8 at 193 K. In the LIFDI-MS spectra of **2b, 2c**, **3a** and **3b** and in the ESI-MS spectrum of **5a**, corresponding molecular ion peaks are detected.

The molecular structures of **2b** and **2c**[10] (Figure 2) reveal dinuclear complexes bearing an E_4 unit, coordinating in an η^2, κ^1 fashion to both $\{L^1Ni\}$ fragments, which are twisted by 37.46(12)° (**2b**) and 37.9882(6)° (**2c**) to each other. In the case of **2c** (use of AsP_3), the arsenic atom is disordered over all four positions, the major isomer, with the arsenic atom at the end of

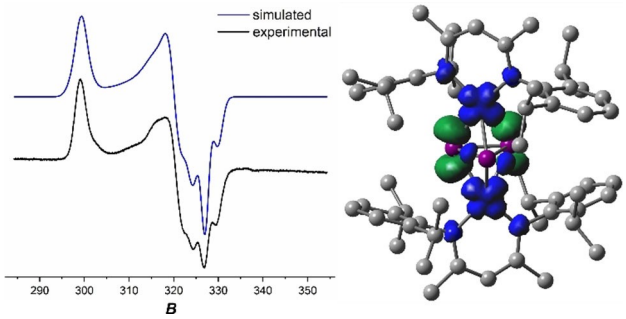

Figure 1. a) X-band EPR spectrum of **3a** (*B* in [mT], frozen toluene solution; 77 K (black), simulation (blue)); b) spin density distribution in **3a**, calculated at the B3LYP/def2-SVP level.

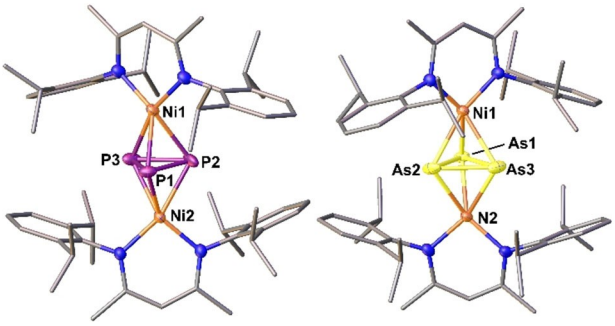

Figure 3. Molecular structures of **3a** (left) and **3b** (right) in the solid state. Thermal ellipsoids are shown at 50% probability level. Hydrogen atoms are omitted for clarity.

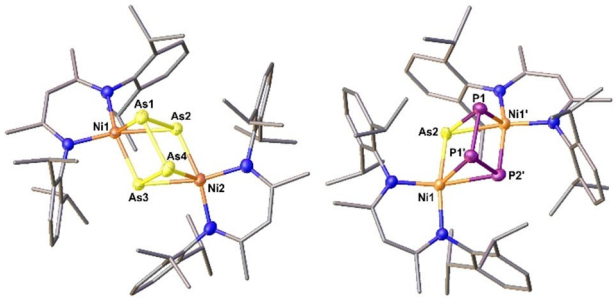

Figure 2. Molecular structures of **2b** (left) and one of the major products of **2c** (right) in the solid state. Thermal ellipsoids are shown at 50% probability level. Hydrogen atoms are omitted for clarity.

Table 1. Comparison of selected atomic distances and angles in **3a**, **3b**, **5a** and **5b** (E = P, As).

Compound	**3a**	**3b**	**5a**	**5b**
d(E–E) [Å]	2.158(10)	2.365(6)	2.1760(10)	2.397(5)
	2.202(11)	2.373(7)	2.1848(10)	2.417(4)
	2.206(14)	2.385(6)	2.2065(10)	2.423(3)
∢ (E–E–E) [°]	58.7(4)	59.6(2)	59.14(4)	59.37(12)
	60.6(4)	59.9(2)	59.80(3)	60.19(11)
	60.8(4)	60.4(2)	60.79(4)	60.44(13)
d(Ni···Ni) [Å]	3.8456(6)	3.9398(6)	3.8169(4)	3.93112(4)
Θ [°]	39.8	39.4	80.11(5)	73.6132(11)

the E_4 chain and the minor isomer with the arsenic atom in the middle of the E_4 chain, is in a ratio of 68:12 (20% are **2a**)[11] in the solid state. The minor isomer is energetically less favored by 13 kJ mol^{-1} to the major isomer (calculated at the BP86/def2-SVP level of theory, see Supporting Information). For **2b**, the As1-As2 and As3-As4 bond distances are 2.4115(5) and 2.4141(5) Å. The As1-As4 distance is slightly shortened (2.3917(5) Å) compared to As1-As2 and As3-As4, while the As2···As3 distance amounts to 2.7192(5) Å and is therefore in a non-bonding area. Compound **2c** shows E–E bond distances between 2.153(8) and 2.422(2) Å. Interestingly, compound $[(Cp^4Ni)_2(\mu\text{-}\eta^2,\kappa^1\text{:}\eta^2,\kappa^1\text{-}As_4)]$ (**F**, $Cp^4 = C_5H^iPr_4$)[12] contains a similar As_4 core and shows longer As–As bond distances between 2.374(3) and 2.435(3) Å. The Ni–E bonds are in the range between 2.3111(7) and 2.4606(6) Å for **2b** and 2.21(3) and 2.378(3) Å for **2c**, which is comparable to **F** (Ni–As_{av} 2.34 Å).

The crystal structure analysis of **3a** and **3b** (Figure 3) reveals dinuclear complexes bearing a *cyclo*-E_3 (E = P, As) ligand as 'middle deck', which is disordered over two positions for **3a** (59:41) and three positions for **3b** (50:25:25) (cf. Supporting Information). The E–E bond distances (Table 1) are in the range between 2.158(10) and 2.206(14) Å (**3a**) or 2.373(7) and 2.599(14) Å (**3b**), respectively. The E–E–E bond angles are in the range of 60°. Both $\{L^1Ni\}$ fragments are twisted to each other by 39.8° (**3a**) and 39.4° (**3b**), respectively. The Ni–E bond lengths are between 2.220(8) and 2.347(8) Å for **3a** and 2.277(8) and 2.521(9) Å for **3b**. The bond distances are comparable to the 33 valence electron complexes $[\{(triphos)Ni\}_2(\mu,\eta^{3:3}\text{-}E_3)][BPh_4]_2$[13] (P–P 2.151(8) to 2.171(7) Å) or $[(L^1Co)_2(\mu,\eta^{3:3}\text{-}E_3)]$[4l,m] (As–As 2.349(3) to 2.563(3) Å). Also, a few other metal complexes are known containing a *cyclo*-E_3 unit which is η^3 coordinated.[4g,14]

In order to evaluate the redox reactivity of **3a** and **3b**, we performed cyclic voltammetry measurements of **3a** (Figure 4) and **3b** (cf. Supporting Information). In THF, a reversible reduction at −1.77 V (**3a**) and −1.91 V (**3b**) and also an

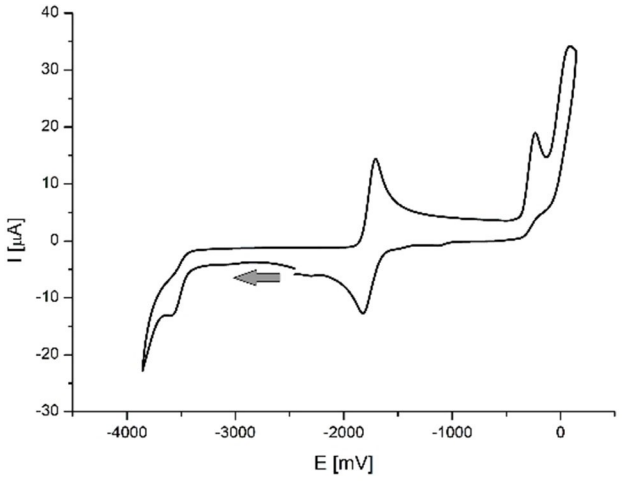

Figure 4. Cyclic voltammogram of **3a** in THF vs. $[Cp_2Fe]/[Cp_2Fe]^+$ (electrolyte: $[^nBu_4N][PF_6]$, scan rate: 100 mV s^{-1}, room temperature).

irreversible oxidation at 0.61 V (**3a**) and −0.42 V (**3b**), respectively, take place (against $[Cp_2Fe]/[Cp_2Fe]^+$). The chemical reduction of **3a** and **3b** was performed with potassium graphite, which was chosen as a suitable reduction agent (redox potential: −2.93 V versus the standard hydrogen electrode), which leads to the formation of $[(K@18\text{-}c\text{-}6)(thf)_3][(L^1Ni)_2(\mu,\eta^{3:3}\text{-}E_3)]$ (E = P (**5a**), As (**5b**)).

The solid-state structures of **5a** and **5b** (Figure 5) are very similar to that of **3a** and **3b** possessing a *cyclo*-E_3 ring which is η^3-coordinated by two $\{L^1Ni\}$ fragments. The *cyclo*-E_3 units are disordered over two positions (ratio 90:10 (**5a**), 61:39 (**5b**)). The E–E bond distances are between 2.130(9) and 2.2065(10) Å (**5a**) and 2.397(5) to 2.423(3) Å (**5b**), respectively, and still intact (Table 1). The Wiberg bond indices (WBIs) underlie this description (WBIs for E–E: **5a** between 0.87 to 1.03; **5b** between 0.93 and 0.98). The E–E–E bond angles are around 60° as also found in compound **3a** and **3b**. However, the structural differences lie in the orientation of the ligands in **3a**, **3b**, **5a** and **5b**. In **3a** and **3b**, the two $\{L^1Ni\}$ fragments are twisted by 39.8° (**3a**) and 39.4° (**3b**) to each other, respectively, in a kind of eclipsed orientation, whereas in **5a** and **5b**, the twist is, with 80.11(5)° (**5a**) and 73.6132(11)° (**5b**), much larger and a more staggered arrangement is present.

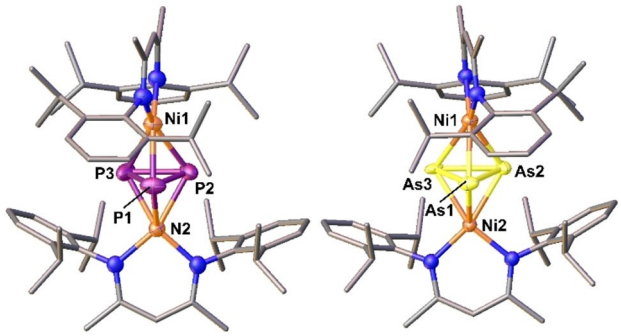

Figure 5. Molecular structures of the anions of **5a** (left) and **5b** (right) in the solid state. Thermal ellipsoids are shown at 50% probability level. Hydrogen atoms, counter ions and solvent molecules are omitted for clarity.

The chemical reduction of **2a** was also performed with potassium graphite. By using two equivalents of KC_8, the dinuclear complex $[(L^1Ni)_2(\mu,\eta^{2:2}\text{-}P_4)][K_2]$ (**4**) could be obtained as brown blocks (Scheme 2). Thus, a conversion and rearrangement to a novel planar *cyclo*-P_4 unit occurred. The molecular structure of **4** reveals an anionic dinuclear complex bearing a *cyclo*-P_4 unit, coordinating in an $\eta^{2:2}$ fashion to two $\{L^1Ni\}$ fragments (Figure 6). The two $\{L^1Ni\}$ fragments are coplanar to each other, and two potassium atoms are stabilized by two opposite dipp groups by $C_{aryl}\cdots K$ interactions. The Ni–P–P angle (cf. Figure 6, angle α) is 101.78(4)°. In the *cyclo*-P_4 unit, there are two different P–P bond lengths. The η^2 coordinated P–P bond length amounts to 2.1360(10) Å (WBI: 1.21), the other P–P bond length is 2.2611(10) Å (WBI: 0.90). In the literature, a few complexes containing a planar *cyclo*-P_4 unit are known which are $\eta^{2:2}$ coordinated.[15] The bonding situation can be considered as being similar to the valence isomer derivative of a tetraphosphabenzene $[\{(^iPr)_2NCP_2\}_2]$ (**G**)[15a] with two single and two P–P double bonds, which was synthesized by Bertrand and coworker. Driess et al. reported the reaction of **1** with sulfur, which leads to a complex containing a related core of sulfur, $[(L^1Ni)_2(\mu,\eta^{2:2}\text{-}S_4)]$.[8b]

Furthermore, the question arose whether the same reactivity could also be observed starting from a reduced Ni_2N_2 nacnac compound. In order to investigate the reactivity of a Ni(0) synthon towards E_4, the formally Ni(0) precursor $[K_2][(L^1Ni)_2(\mu,\eta^{1:1}\text{-}N_2)]$ (**6**) was synthesized and crystallized as purple needles in crystalline yields of 47%.

In the ^1H NMR spectrum of **6**, the typical signals for the β-diiminato ligand can be observed. The X-ray structure of **6** (Figure 7) consists of two $\{L^1Ni\}$ fragments bridged by a N_2 unit, which additionally coordinates to two potassium ions. The

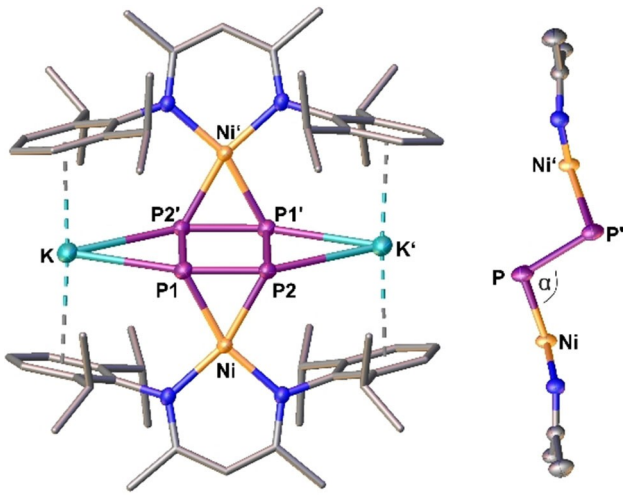

Figure 6. Molecular structure of **4** (left) in the solid state and side view (right) Isopropyl groups (for right), solvent molecules and hydrogen atoms are omitted for clarity. Thermal ellipsoids are shown at 50% probability level.

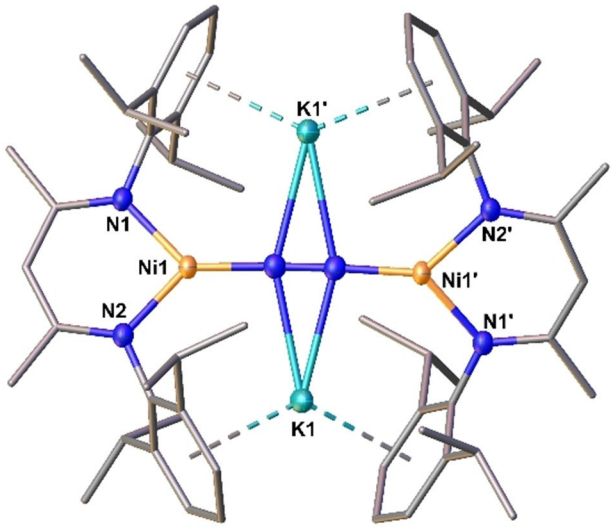

Figure 7. Molecular structure of **6** in the solid state. Thermal ellipsoids are shown at 50% probability level. Hydrogen atoms are omitted for clarity.

potassium ions are coordinated by the aromatic π system of the dipp substituent. The N–N bond distance with 1.195(5) Å corresponds to an N–N double bond (N_2H_2: 1.230 Å[16]) and the N–N stretching band in the Raman spectrum is detected at 1572 cm^{-1}. Complexes similar to **6** are known in the literature and the N–N bond distances and stretching bands show that the N_2 unit in **6** can be regarded as a N_2^{2-} unit.[3a,b,17]

In order to investigate if this formally Ni(0) synthon leads in reactions with E_4 (E = P, As) to similar products or not as its Ni(I) derivative, **6** was reacted with white phosphorus and yellow arsenic at room temperature in the presence of 18-crown-6 (18-c-6) or cryptant (crypt). Adding 18-c-6 or crypt to **6** before E_4 leads to the formation of $[(K@X)(thf)_2][L^1Ni(\eta^{1:1}\text{-}E_4)]$ (E = P, X = 18-c-6 (**7a**), E = As, X = 18-c-6 or crypt (**7b**)), which are isolated as air-sensitive orange (**7a**) or reddish-brown (**7b**) needles in crystalline yields of 42% (**7a**) and 39% (**7b**, X = crypt), respectively (Scheme 3). If **6** is reacted with yellow arsenic and 18-c-6 is added afterwards, the formation of [(K@18-crown-6)$(thf)_3$][$(L^1Ni)_2(\mu,\eta^{3:3}\text{-}As_3)$] (**5b**) in crystalline yields of 30% occurs (Scheme 3), which, for phosphorus, could not be observed (formation of **7a**). Thus, the formation of **7a** and **7b** shows the difference between the use of a Ni(0) or Ni(I) synthon.

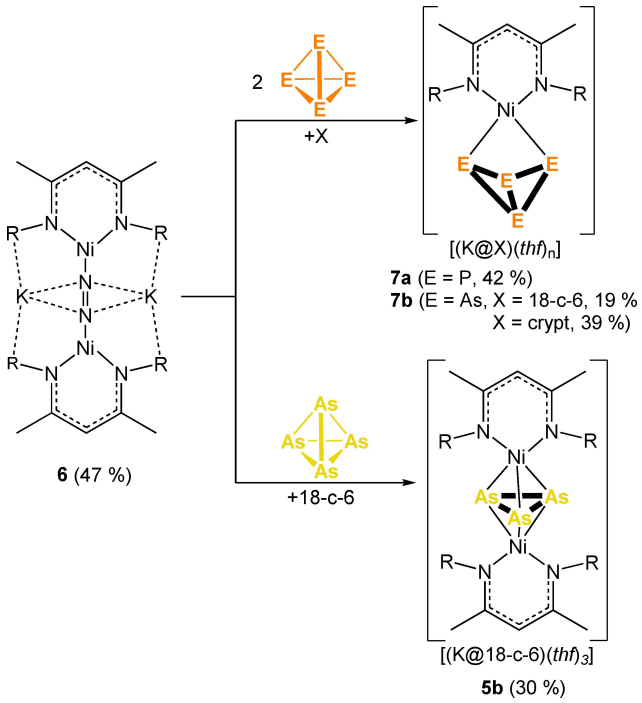

Scheme 3. Reaction of **6** with E_4 (E = P, As). R = dipp = 2,6-diisopropylphenyl, X = 18-c-6, crypt.

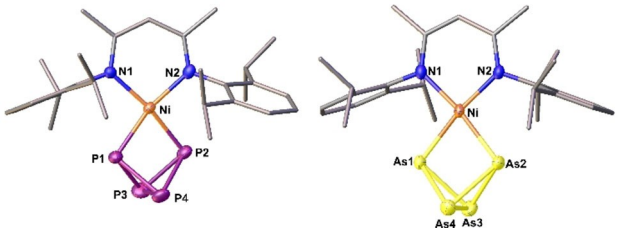

Figure 8. Molecular structure of the anions of **7a** and **7b** in the solid state. Thermal ellipsoids are shown at 50% probability level. Hydrogen atoms and counter ions are omitted for clarity.

The $^{31}P\{^1H\}$ NMR spectrum of **7a** in thf-d_8 shows two triplets at −378.3 and −212.9 ppm ($^1J_{PP}$ = 133 Hz). The ^1H NMR spectrum of **7b** in thf-d_8 is very similar to the one of **7a**.

The molecular structures of **7a** and **7b** (Figure 8) reveal anionic mononuclear complexes bearing an E_4 butterfly ligand, coordinating in an $\eta^{1:1}$ fashion to the $\{L^1Ni\}$ fragment. The six-membered NiN_2C_3 ring is twisted by 14.8847(1)° for **7a** and 0.78(4)° for **7b** to the E1–Ni–E2 plane. With 2.6759(15) (**7a**) and 2.8963(3) Å (**7b**), the E1···E2 distances lie in a non-bonding area. The E–E bond lengths are between 2.2115(16) and 2.2282(17) Å for **7a** and 2.4506(4) and 2.4687(3) Å for **7b**, except for the E3–E4 bond length which is shortened to 2.1567(18) (**7a**) and 2.3908(4) Å (**7b**). This is in accordance with other butterfly complexes. Interestingly, the Driess group proposed the occurrence of a neutral compound $[L^1Ni(\eta^2\text{-}P_4)]$ with an η^2 side on coordinated P_4 tetrahedra by high-resolution ESI MS data.[4c] With compounds **7a** and **7b**, anionic species are formed and completely characterized.

Conclusion

In summary, we have shown the different reactivities of β-diiminato Ni(I) and Ni(0) complexes towards white phosphorus, yellow arsenic and the interpnictogen compound AsP_3. The reactions of $[(L^1Ni)_2tol]$ (**1**) with white phosphorus and yellow arsenic as well as AsP_3 are temperature-dependent. Thus, the homobimetallic complexes $[(L^1Ni)_2(\mu\text{-}\eta^2,\kappa^1\text{:}\eta^2,\kappa^1\text{-}E_4)]$ (E = As (**2b**), AsP_3 (**2c**)) and $[(L^1Ni)_2(\mu,\eta^{3:3}\text{-}E_3)]$ (E = P (**3a**), As (**3b**)) are formed, of which **3a** and **3b** are paramagnetic. DFT calculations exhibit that the spin density is delocalized over both nickel atoms and two pnictogen atoms. To investigate the redox reactivity of **3a** and **3b**, cyclic voltammetry measurements were performed and [(K@18-crown-6)$(thf)_3$][$(L^1Ni)_2(\mu,\eta^{3:3}\text{-}E_3)$] (E = P (**5a**), As (**5b**)) was isolated after experimental reduction. In contrast, the chemical reduction of **2a** leads to an unusual planarization of the initial Ni_2P_4-prism. Furthermore, the reaction of E_4 (E = P, As) with a formally Ni(0) synthon leads to the formation of the novel monoanionic compounds $[(K@X)thf)_2][L^1Ni(\eta^{1:1}\text{-}E_4)]$ (E = P, X = 18-c-6 (**7a**), As, X = crypt (**7b**)), which shows the differences between the use of a Ni(I) and a Ni(0) synthon. Additionally, an alternative synthetic approach for **5b** was found, using **6** as starting material, but by adding 18-c-6 after the reaction with As_4. The results show the broad variety of different E_n-structural motifs formed with nickel nacnac complexes in the conversion of E_4 and underline the great potential of the use of Ni(0) synthons in synthesis.

X-ray crystallography

Deposition Number(s) 2109927 (**2b**), 2109928 (**2c**), 2109929 (**3a**), 2109930 (**3b**), 2109931 (**4**), 2109932 (**5a**), 2109933 (**5b**), 2109934(**6**), 2109935 (**7a**), 2109936 (**7b**) contain(s) the supplementary crystallographic data for this paper. These data are provided free of charge by the joint Cambridge Crystallographic Data Centre and Fachinformationszentrum Karlsruhe Access Structures service.

Acknowledgements

This work was supported by the Deutsche Forschungsgemeinschaft within the project Sche 384/40-1. M.P. is grateful to the Fonds der Chemischen Industrie for a PhD fellowship. Open Access funding enabled and organized by Projekt DEAL.

Conflict of Interest

The authors declare no conflict of interest.

Keywords: activation · reduction · transition metal · white phosphorus · yellow arsenic

[1] a) R. A. Henderson, *Trans. Met. Chem.* **1990**, *15*, 330–336; b) X. Yin, J. R. Moss, *Coord. Chem. Rev.* **1999**, *181*, 27–59; c) G. C. Welch, R. R. S. Juan, J. D. Masuda, D. W. Stephan, *Science* **2006**, *314*, 1124–1126; d) V. P. Indrakanti, J. D. Kubicki, H. H. Schobert, *Energy Environ. Sci.* **2009**, *2*, 745–758; e) D. W. Stephan, *Dalton Trans.* **2009**, 3129–3136; f) N. Hazari, *Chem. Soc. Rev.* **2010**, *39*, 4044–4056; g) C. Chow, M. Taoufik, E. A. Quadrelli, *Eur. J. Inorg. Chem.* **2011**, *2011*, 1349–1359; h) M. Behrens, *Angew. Chem. Int. Ed.* **2014**, *53*, 12022–12024; *Angew. Chem.* **2014**, *126*, 12216–12218; i) I. Mellone, F. Bertini, L. Gonsalvi, A. Guerriero, M. Peruzzini, *Chimia* **2015**, *69*, 331–338; j) Z. R. Turner, *Inorganics* **2015**, *3*, 597–635; k) D. M. Ermert, L. J. Murray, *Dalton Trans.* **2016**, *45*, 14499–14507.

[2] a) L. Bourget-Merle, M. F. Lappert, J. R. Severn, *Chem. Rev.* **2002**, *102*, 3031–3066; b) Y.-C. Tsai, *Coord. Chem. Rev.* **2012**, *256*, 722–758.

[3] a) J. M. Smith, R. J. Lachicotte, K. A. Pittard, T. R. Cundari, G. Lukat-Rodgers, K. R. Rodgers, P. L. Holland, *J. Am. Chem. Soc.* **2001**, *123*, 9222–9223; b) J. M. Smith, A. R. Sadique, T. R. Cundari, K. R. Rodgers, G. Lukat-Rodgers, R. J. Lachicotte, C. J. Flaschenriem, J. Vela, P. L. Holland, *J. Am. Chem. Soc.* **2006**, *128*, 756–769; c) D. J. E. Spencer, A. M. Reynolds, P. L. Holland, B. A. Jazdzewski, C. Duboc-Toia, L. Le Pape, S. Yokota, Y. Tachi, S. Itoh, W. B. Tolman, *Inorg. Chem.* **2002**, *41*, 6307–6321; d) D. E. DeRosha, B. Q. Mercado, G. Lukat-Rodgers, K. R. Rodgers, P. L. Holland, *Angew. Chem. Int. Ed.* **2017**, *56*, 3211–3215; *Angew. Chem.* **2017**, *129*, 3259–3263; e) S. Yao, E. Bill, C. Milsmann, K. Wieghardt, M. Driess, *Angew. Chem. Int. Ed.* **2008**, *47*, 7110–7113; *Angew. Chem.* **2008**, *120*, 7218–7221.

[4] a) Y. Peng, H. Fan, H. Zhu, H. W. Roesky, J. Magull, C. E. Hughes, *Angew. Chem. Int. Ed.* **2004**, *43*, 3443–3445; *Angew. Chem.* **2004**, *116*, 3525–3527; b) G. Prabusankar, A. Doddi, C. Gemel, M. Winter, R. A. Fischer, *Inorg. Chem.* **2010**, *49*, 7976–7980; c) S. Yao, Y. Xiong, C. Milsmann, E. Bill, S. Pfirrmann, C. Limberg, M. Driess, *Chem. Eur. J.* **2010**, *16*, 436–439; d) B. L. Tran, M. Singhal, H. Park, O. P. Lam, M. Pink, J. Krzystek, A. Ozarowski, J. Telser, K. Meyer, D. J. Mindiola, *Angew. Chem. Int. Ed.* **2010**, *49*, 9871–9875; *Angew. Chem.* **2010**, *122*, 10067–10071; e) C. Camp, L. Maron, R. G. Bergman, J. Arnold, *J. Am. Chem. Soc.* **2014**, *136*, 17652–17661; f) M. Arrowsmith, M. S. Hill, A. L. Johnson, G. Kociok-Köhn, M. F. Mahon, *Angew. Chem. Int. Ed.* **2015**, *54*, 7882–7885; *Angew. Chem.* **2015**, *127*, 7993–7996; g) B. Pinter, K. T. Smith, M. Kamitani, E. M. Zolnhofer, B. L. Tran, S. Fortier, M. Pink, G. Wu, B. C. Manor, K. Meyer, M.-H. Baik, D. J. Mindiola, *J. Am. Chem. Soc.* **2015**, *137*, 15247–15261; h) F. Spitzer, M. Sierka, M. Latronico, P. Mastrorilli, A. V. Virovets, M. Scheer, *Angew. Chem. Int. Ed.* **2015**, *54*, 4392–4396; *Angew. Chem.* **2015**, *127*, 4467–4472; i) S. Yao, T. Szilvasi, N. Lindenmaier, Y. Xiong, S. Inoue, M. Adelhardt, J. Sutter, K. Meyer, M. Driess, *Chem. Commun.* **2015**, *51*, 6153–6156; j) F. Spitzer, C. Graßl, G. Balázs, E. M. Zolnhofer, K. Meyer, M. Scheer, *Angew. Chem. Int. Ed.* **2016**, *55*, 4340–4344; *Angew. Chem.* **2016**, *128*, 4412–4416; k) F. Hennersdorf, J. Frötschel, J. J. Weigand, *J. Am. Chem. Soc.* **2017**, *139*, 14592–14604; l) F. Spitzer, C. Graßl, G. Balázs, E. Mädl, M. Keilwerth, E. M. Zolnhofer, K. Meyer, M. Scheer, *Chem. Eur. J.* **2017**, *23*, 2716–2721; m) F. Spitzer, G. Balázs, C. Graßl, M. Keilwerth, K. Meyer, M. Scheer, *Angew. Chem. Int. Ed.* **2018**, *57*, 8760–8764; *Angew. Chem.* **2018**, *130*, 8896–8900; n) F. Spitzer, G. Balázs, C. Graßl, M. Scheer, *Chem. Commun.* **2020**, *56*, 13209–13212.

[5] The expression "realgar-type" for the tricyclo[3.3.0.$0^{3,7}$]octaphosphane ligand based on its analogy to the isosturctural $[As_4S_4]$ molecule.

[6] S. Yao, N. Lindenmaier, Y. Xiong, S. Inoue, T. Szilvási, M. Adelhardt, J. Sutter, K. Meyer, M. Driess, *Angew. Chem. Int. Ed.* **2015**, *54*, 1250–1254; *Angew. Chem.* **2015**, *127*, 1266–1270.

[7] D. J. Mindiola, *Angew. Chem. Int. Ed.* **2009**, *48*, 6198–6200, *Angew. Chem.* **2009**, *121*, 6314–6316.

[8] a) S. Yao, Y. Xiong, X. Zhang, M. Schlangen, H. Schwarz, C. Milsmann, M. Driess, *Angew. Chem. Int. Ed.* **2009**, *48*, 4551–4554; *Angew. Chem.* **2009**, *121*, 4621–4624; b) S. Yao, C. Milsmann, E. Bill, K. Wieghardt, M. Driess, *J. Am. Chem. Soc.* **2008**, *130*, 13536–13537.

[9] By stirring a solution of **2b** with potassium graphit, the reaction mixture turned reddish-brown, as in the case of phosphorus. Unfortunately, a crystallisation of this reduced compound failed, regardless on numerous attempts.

[10] In the asymmetric unit are three molecules of **2c**. We discuss here only one selected molecule.

[11] The starting material AsP_3 is contaminated with P_4.

[12] O. J. Scherer, J. Braun, P. Walther, G. Wolmershäuser, *Chem. Ber.* **1992**, *125*, 2661–2665.

[13] M. Di Vaira, S. Midollini, L. Sacconi, *J. Am. Chem. Soc.* **1979**, *101*, 1757–1763.

[14] a) M. Di Vaira, C. A. Ghilardi, S. Midollini, L. Sacconi, *J. Am. Chem. Soc.* **1978**, *100*, 2550–2551; b) E. Mädl, G. Balázs, E. V. Peresypkina, M. Scheer, *Angew. Chem. Int. Ed.* **2016**, *55*, 7702–7707; *Angew. Chem.* **2016**, *128*, 7833–7838; c) M. Caporali, L. Gonsalvi, A. Rossin, M. Peruzzini, *Chem. Rev.* **2010**, *110*, 4178–4235; d) S. Du, J. Yin, Y. Chi, L. Xu, W.-X. Zhang, *Angew. Chem. Int. Ed.* **2017**, *56*, 15886–15890; *Angew. Chem.* **2017**, *129*, 16102–16106.

[15] a) Y. Canac, D. Bourissou, A. Baceiredo, H. Gornitzka, W. W. Schoeller, G. Bertrand, *Science* **1998**, *279*, 2080–2082; b) S. Du, J. Yang, J. Hu, Z. Chai, G. Luo, Y. Luo, W.-X. Zhang, Z. Xi, *J. Am. Chem. Soc.* **2019**, *141*, 6843–6847.

[16] P. Pyykkö, M. Atsumi, *Chem. Eur. J.* **2009**, *15*, 12770–12779.

[17] a) K. Ding, A. W. Pierpont, W. W. Brennessel, G. Lukat-Rodgers, K. R. Rodgers, T. R. Cundari, E. Bill, P. L. Holland, *J. Am. Chem. Soc.* **2009**, *131*, 9471–9472; b) S. Pfirrmann, C. Limberg, C. Herwig, R. Stößer, B. Ziemer, *Angew. Chem. Int. Ed.* **2009**, *48*, 3357–3361; *Angew. Chem.* **2009**, *121*, 3407–3411.

Manuscript received: September 15, 2021
Accepted manuscript online: November 3, 2021
Version of record online: November 23, 2021

